

**PAPER****Ultrafast artificial intelligence: machine learning with atomic-scale quantum systems****OPEN ACCESS****RECEIVED**

26 April 2024

REVISED

22 August 2024

ACCEPTED FOR PUBLICATION

28 August 2024

PUBLISHED

12 September 2024

Original Content from
this work may be used
under the terms of the
[Creative Commons
Attribution 4.0 licence](#).

Any further distribution
of this work must
maintain attribution to
the author(s) and the title
of the work, journal
citation and DOI.

Thomas Pfeifer^{1,*} , Matthias Wollenhaupt^{2,*}  and Manfred Lein^{3,*} ¹ Max-Planck-Institut für Kernphysik, 69117 Heidelberg, Germany² Institut für Physik, Carl von Ossietzky Universität Oldenburg, Carl-von-Ossietzky-Straße 9-11, Oldenburg 26129, Germany³ Leibniz Universität Hannover, Institut für Theoretische Physik, Appelstraße 2, 30167 Hannover, Germany

* Authors to whom any correspondence should be addressed.

E-mail: thomas.pfeifer@mpi-hd.mpg.de, matthias.wollenhaupt@uni-oldenburg.de and lein@itp.uni-hannover.de**Keywords:** quantum dynamics, ultrafast, artificial intelligence, electron dynamics, atoms**Abstract**

We train a model atom to recognize pixel-drawn digits based on hand-written numbers in the range 0–9, employing intense light–matter interaction as a computational resource. For training, the images of the digits are converted into shaped laser pulses (data input pulses). Simultaneously with an input pulse, another shaped pulse (program pulse), polarized in the orthogonal direction, is applied to the atom and the system evolves quantum mechanically according to the time-dependent Schrödinger equation. The purpose of the optimal program pulse is to direct the system into specific atomic final states (classification states) that correspond to the input digits. A success rate of about 40% is achieved when using a basic optimization scheme that might be limited by the computational resources for finding the optimal program pulse in a high-dimensional search space. Our key result is the demonstration that the laser-programmed atom is able to generalize, i.e. successful classification is not limited to the training examples, but also the classification of previously unseen images is improved by training. This atom-sized machine-learning image-recognition scheme operates on time scales down to tens of femtoseconds, is scalable towards larger (e.g. molecular) systems, and is readily reprogrammable towards other learning/classification tasks. An experimental implementation of the scheme using ultrafast polarization pulse shaping and differential photoelectron detection is within reach.

1. Introduction

Artificial intelligence (AI) is an area of growing interest and with an enormous range of applications, due to recent successes and breakthroughs in deep learning, enabled by the steady increase in (classical) computational power [1, 2]. Within this field, image recognition, i.e. the classification of different but conceptually equivalent (input) images into unique (output) categories, has been one of the prime applications of AI and machine learning for many years [3]. A key component of machine learning is the ability of the trained system to generalize [4–6], i.e. to correctly classify input data that was not part of the training data.

With recent advances in optical science and technology, in particular optical neuromorphic hardware [7], it has recently been possible to accelerate image recognition to sub-nanosecond timescales [8]. Here, the operation timescale is determined by the speed of light at which information propagates in microscopic waveguides on the chip, and is thus directly proportional to its size: The smaller the device and the computational units, the faster the clock rates for the recognition operations will become. The fundamental limit to further minimization is the atomic scale.

In atomic and molecular physics, extreme timescales down to femtoseconds and even attoseconds are currently being explored and controlled by measuring and steering the motion of one, two, or more

electrons [9–14] with lasers. Atomic states are excited and coupled on ultrafast (femtosecond) time scales [15], providing a quantum analogue of neurons (quantum states) and axons (laser coupling between states). Ground-state atoms and molecules are fully quantum-correlated systems and therefore entanglement arises naturally when these systems fragment into two or more particles [16, 17], e.g. due to photoionization or dissociation. Control of entangled states using attosecond and femtosecond laser pulses has also been addressed recently [18–21]. The natural question is whether atoms and their interaction with intense laser light can be used as a high-speed computational resource in applications such as machine learning for image recognition. This question has recently been addressed for the case of two-class recognition of hand-written pixel-drawn digits and three-class recognition of iris-flower types, using the process of high-order harmonic generation and thus an optical output channel [22].

In the present work, we investigate whether an atom could at the same time act as a quantum processor *and* readout register for machine learning, mapping two-dimensional images of digits directly onto atomic quantum states, referred to as classification states in the following. The latter could then be either read out or serve as input to subsequent (quantum) processing tasks. Our approach is to be distinguished from recent developments referred to as quantum machine learning [23, 24], where the ultimate goal is to train quantum computing devices to perform quantum tasks, and also from the earlier proposals to mimic specific quantum gates in laser-driven molecules [25–27] or Rydberg atomic systems [28]. In our case, we train quantum systems directly and demonstrate generalization capability, without the intention of developing a quantum algorithm as sequence of established quantum gates. Being based on the time evolution of a quantum system, our scheme benefits from the same quantum effects that can enable quantum speedup in the framework of quantum computing, see the discussions specifically in the context of classification tasks [29, 30].

2. Methodology

In the following, we introduce our scheme and present the results of a model-atom simulation as a proof of principle. Both the input data and the code that processes the data are supplied to the atom in the form of shaped femtosecond light pulses, namely input/data(id) pulse and program/code(pc) pulse (see figure 1). Due to the ultrafast time scale, incoherent coupling to the environment can be neglected, i.e. the dynamics of the atom is described by the time evolution of a pure state evolving according to the time-dependent Schrödinger equation (TDSE) $i\partial_t\Psi = \mathcal{H}\Psi$ (atomic units are used unless stated otherwise). We show that the atom can be successfully trained, despite a huge parameter space for the optical pc pulse, which is obtained by an evolutionary optimization procedure [31]. We expect that the training approach will be significantly improved in the future, e.g. by using more suitable parameterizations for the program pulse and advanced statistical methods based on Bayesian inference. Finding the optimal pc pulse, which is initially unknown, can also be understood and formulated as a reinforcement learning problem [32]. After completed training, the laser-driven atom is able to take its decisions within femtoseconds and may therefore be viewed as ultrafast AI, where the term ‘ultrafast’ refers to the time scale of the system behavior, not necessarily to the learning process. An experimental implementation would involve a gas-jet target, supplying continuously fresh atoms, so that the quantum-mechanical time evolution always starts from the same initial state. Therefore, unwanted heating of the quantum system is not an issue.

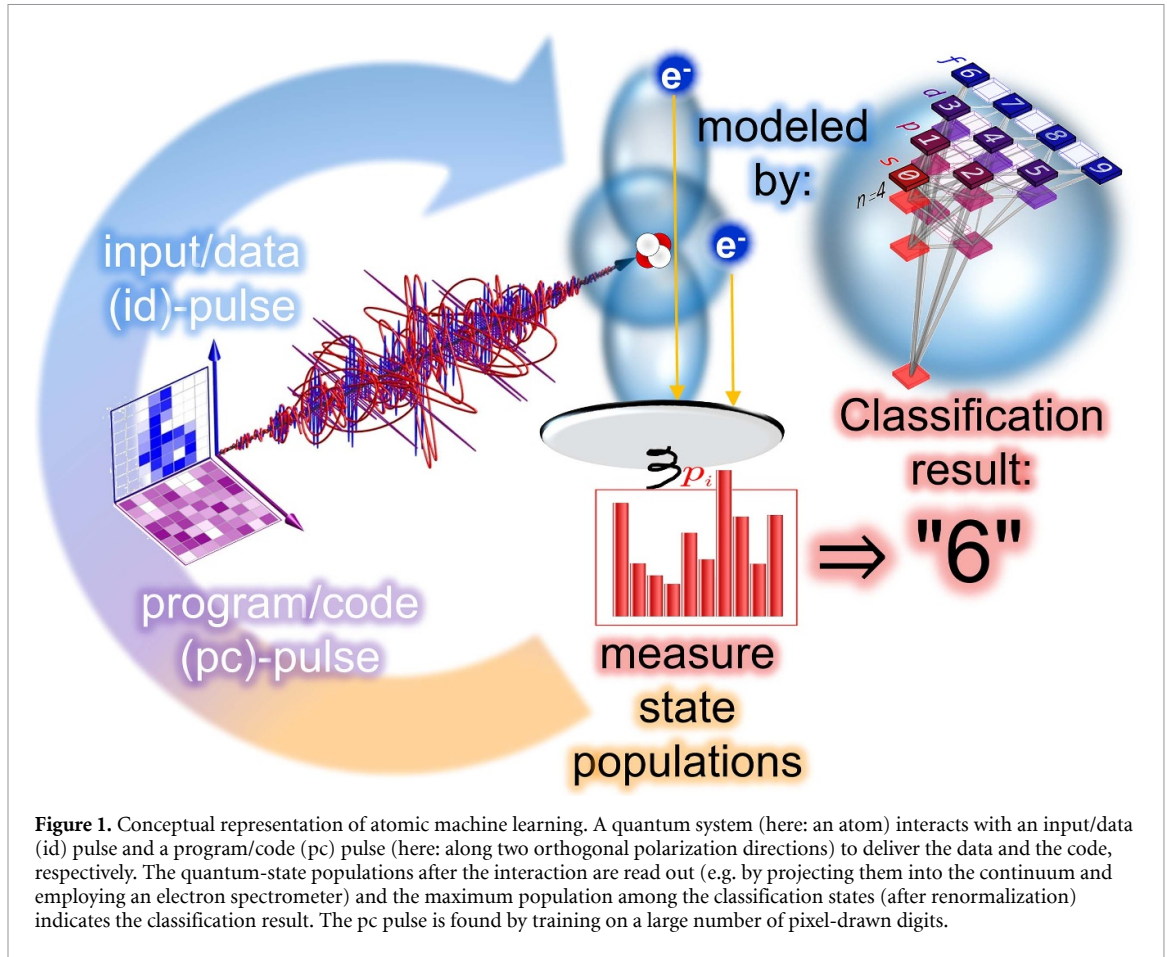
3. Atomic model

In our simulations, we employ a multi-level Hamiltonian \mathcal{H}_0 to describe the atom, which is dipole coupled to an external arbitrarily polarized time-dependent laser field vector $\mathbf{E}(t) = E_x(t)\mathbf{e}_x + E_y(t)\mathbf{e}_y$ with Cartesian unit vectors $\mathbf{e}_x, \mathbf{e}_y$. The interacting Hamiltonian thus reads

$$\mathcal{H} = \mathcal{H}_0 + \mathcal{V}_x E_x(t) + \mathcal{V}_y E_y(t). \quad (1)$$

Using a 20-level model with basis states 1s, 2s, 2p_{-1,1}, 3s, 3p_{-1,1}, 3d_{-2,0,2}, 4s, 4p_{-1,1}, 4d_{-2,0,2}, 4f_{-3,-1,1,3}, we have

$$\mathcal{H}_0 = \begin{pmatrix} E_{1s} & 0 & 0 & & \\ 0 & E_{2s} & 0 & & \\ 0 & 0 & E_{2p} & & \\ & & & \ddots & \end{pmatrix}, \quad (2)$$



$$\mathcal{V}_x = \begin{pmatrix} 0 & 0 & a & -a \\ 0 & 0 & a & -a \\ a & a & 0 & 0 \\ -a & -a & 0 & 0 \\ \vdots & \vdots & \vdots & \vdots \end{pmatrix}, \quad (3)$$

and

$$\mathcal{V}_y = \begin{pmatrix} 0 & 0 & -ia & -ia \\ 0 & 0 & -ia & -ia \\ ia & ia & 0 & 0 \\ ia & ia & 0 & 0 \\ \vdots & \vdots & \vdots & \vdots \end{pmatrix}. \quad (4)$$

For simplicity, the energies are chosen as $E_{nl} = -1/(n+1)^2$. The coupling matrix elements read $\mathcal{V}_x^{jk} = \langle l, m | \sin \theta \cos \phi | l', m' \rangle$ and $\mathcal{V}_y^{jk} = \langle l, m | \sin \theta \sin \phi | l', m' \rangle$, where the index j corresponds to the state $|n, l, m\rangle$, the index k corresponds to the state $|n', l', m'\rangle$, and $|l, m\rangle$ are angular momentum states. These matrix elements are the angular factors in the x and y components of the dipole transition elements, written in angular-momentum representation, using $x = r \sin \theta \cos \phi$ and $y = r \sin \theta \sin \phi$, where θ and ϕ are the polar angle and the azimuthal angle, respectively. The radial integrals have been set to unity to emphasize the generic character of the model. This means that, for example, the number a appearing in equation (3) is $a = \langle 0, 0 | \sin \theta \cos \phi | 1, -1 \rangle$. The $1s$ state $|1, 0, 0\rangle$ is taken as the initial state for the time evolution. As the system is strongly perturbed by the applied laser fields, giving rise to large generalized Rabi frequencies that substantially modify the dressed-state energies, the exact field-free energies of the states have limited relevance for the laser-induced dynamics.

The orthogonally-polarized shaped laser fields [27] E_x and E_y encode the input data (pixel-drawn digits) in the x -component and the program data in the y -component. Each digit image and each program consists of 64 values. Essentially, we translate these values into the phases of 64 different frequencies, from which a

pulse is composed. In detail, the encoding is implemented as follows. We start from a \cos^2 -shaped spectral amplitude

$$\tilde{E}(\omega) = \tilde{E}_0 \cos^2\left(\frac{\omega - \omega_0}{\Omega} \pi\right), \quad (5)$$

$$\omega_0 - \Omega/2 \leq \omega \leq \omega_0 + \Omega/2, \quad (6)$$

where ω is the frequency, the spectral range is $\Omega = \pi/32$ a.u. and the central frequency ω_0 corresponds to a laser wavelength of 800 nm. The time-dependent field $E(t)$ is then obtained as a Fourier-synthesis of 64 components, multiplied by an additional \cos^2 temporal envelope to restrict the pulse to a finite total duration T , i.e.

$$E(t) = \cos^2(t\pi/T) \sum_{j=0}^{63} \tilde{E}(\omega_j) \cos(-\omega_j t + \varphi_j), \quad (7)$$

$$-T/2 \leq t \leq T/2 \quad (8)$$

with

$$\omega_j = \omega_0 + (j - 31) \Delta\omega, \quad \Delta\omega = 2\pi/T, \quad (9)$$

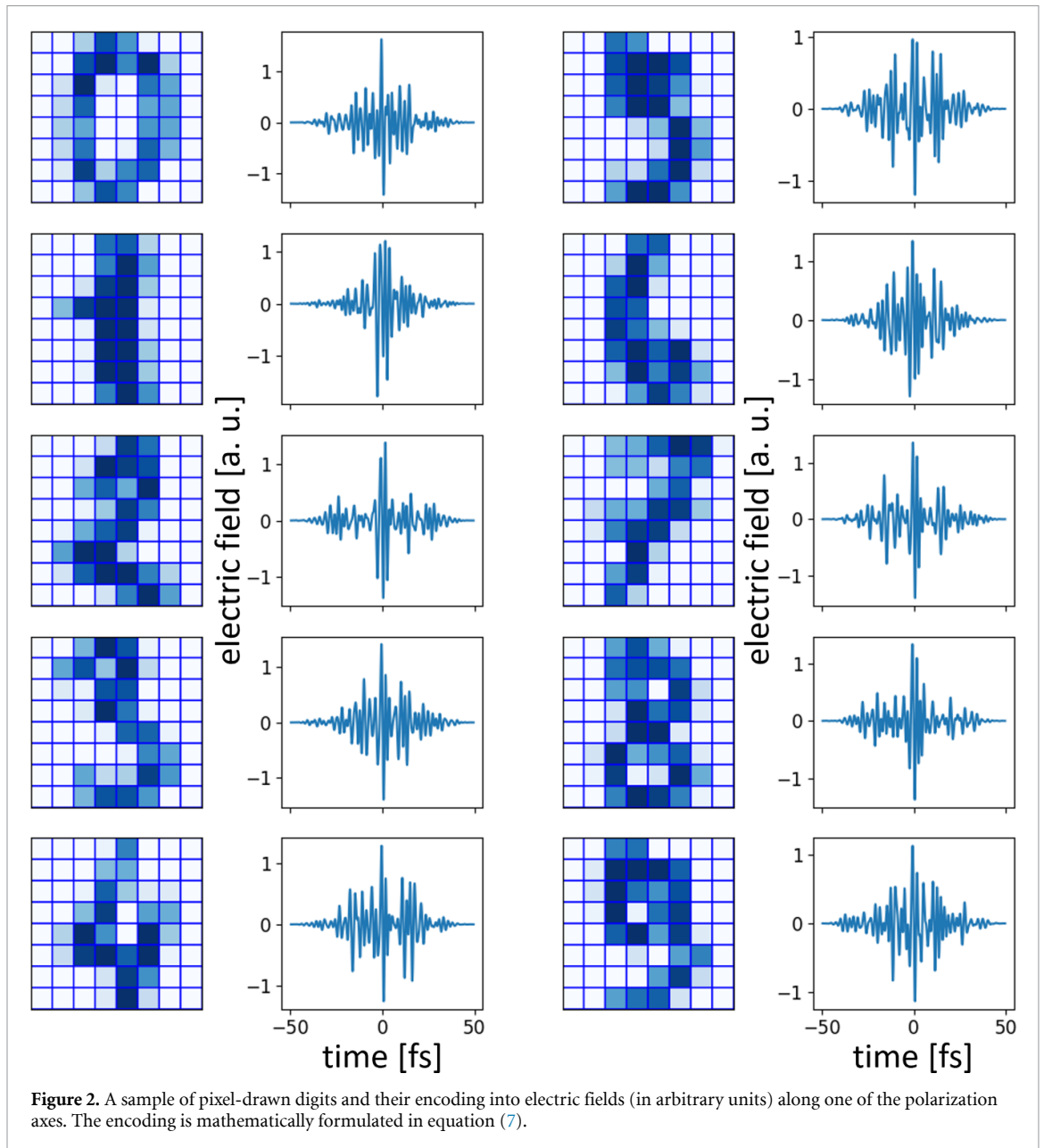
$$T = 4096 \text{ a.u.}, \quad (10)$$

$$\varphi_j = -3\nu_j \text{ rad.} \quad (11)$$

Here, ν_j (in the range $0 \leq \nu_j \leq 1$) are the 64 data values describing either the input or the program. In the case of the input, ν_j are the pixel intensities of hand-written pixel-drawn digits from the scikit-learn python package [28], 8×8 pixel representation, processed column-wise from the lower right to the upper left corner. Examples of this parameterization are shown in figure 2.

The TDSE is then solved numerically by a split-step operator approach [33–35] with a time step of 1 a.u., and the final state populations p_i ('output') are read out for each pair of 100 input and 20 program fields. Among the excited states, we select 10 classification states (namely, all dipole-accessible 4s, 4p, 4d, 4f states) to represent the digits from '0' to '9'. These energetically high-lying states would also be most easily accessible and discernible for probing by single- or few-photon ionization in an experimental implementation. Because not all classification states will be equally populated for an arbitrary set of pulses, we renormalize the final populations of the classification states as $P_j = p_j/p_{0j}$ ($j = 0, \dots, 9$), where p_{0j} is obtained by applying a set of random pc pulses and reading out their final state populations. This renormalization strategy makes the scheme robust against the particular choice of quantum system. Any experimental implementation of the scheme needs to be performed on an ensemble of atoms, in order to perform not just a single measurement (determining the state $|n, l, m\rangle$ of a single atom), but to obtain the ensemble average, i.e. the probabilities of finding an atom in any of the target states. The classification state with the highest renormalized population is then identified as the classification output between '0' and '9'.

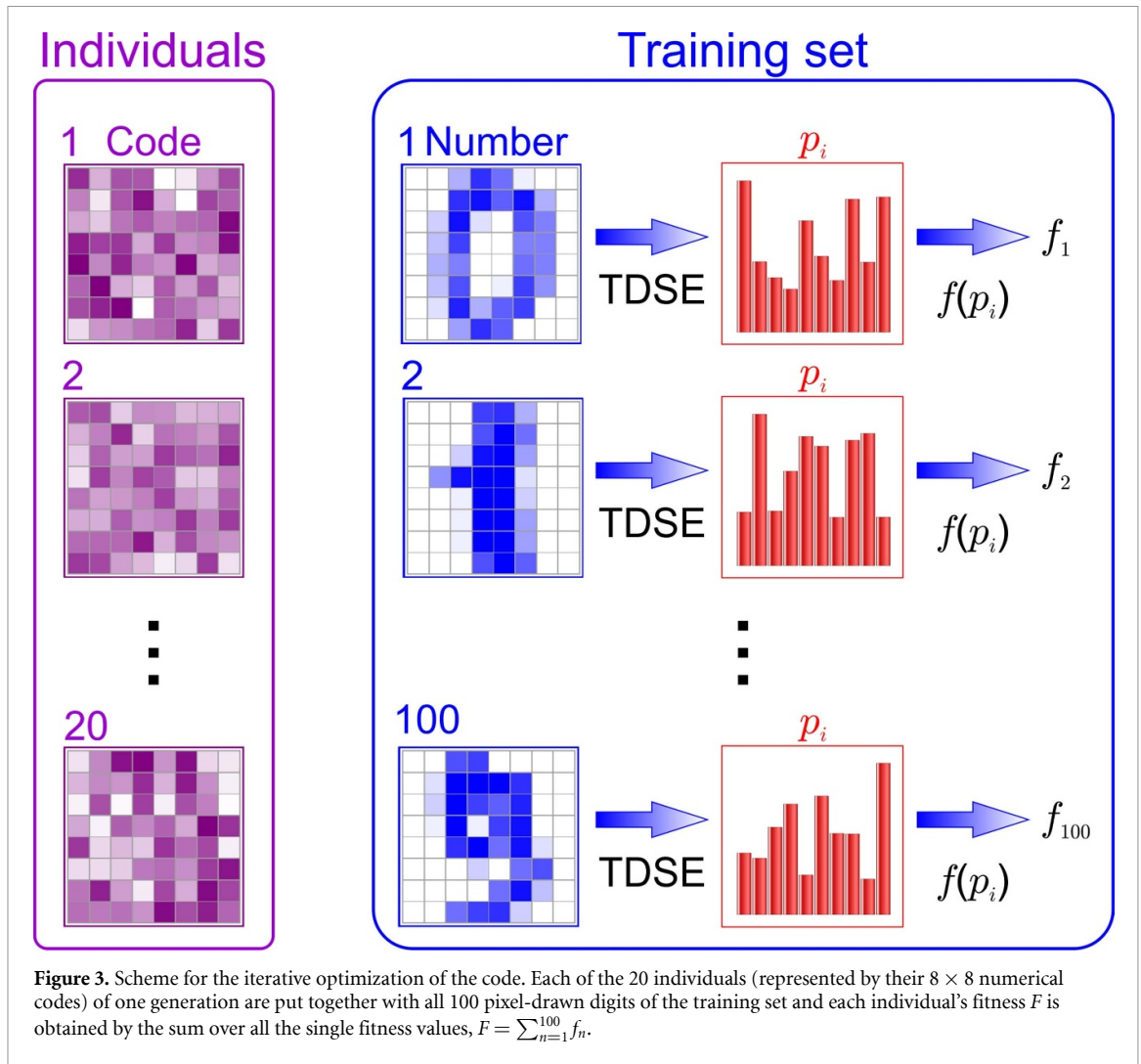
We assign to each program field a fitness $F = 3N + P$ with N the number of matches between the input (pixel-drawn digit) and classification output (state with highest renormalized population). The term P is included to reward those pulses leading to particularly high populations of the correct classification states: $P = \sum_{n=1}^{100} P_{j(n)}^{(n)}$ is the sum over the renormalized populations $P_{j(n)}^{(n)}$ for each of the 100 input fields of the training set, with $j(n)$ being the correct classification state for the n th input field. The program fields are then iteratively optimized by an evolutionary algorithm [36] to maximize their fitness. The goal is to find an optimal program field that guarantees correct classification of all training digits. The evolutionary algorithm employed here to train the model atom uses a population size of 20 individuals, each represented by an array of 64 numbers, which determine the spectral phase of the pc pulse in the same way as for the input pulses. For each individual pc pulse its fitness is calculated by applying the pulse to 100 pixel-drawn digits from the training set, as shown in figure 3. The best pc pulse is always kept for the next generation while the remaining 19 individuals are obtained by a combination of cross-over and mutation (using random numbers) of the previous 64-number representations.



4. Results and conclusion

The results of three sample optimization runs are shown in figure 4. While the proportion of correctly classified digits generally rises throughout the optimizations (black line), it is particularly interesting to observe the correlated increase of the success rate on the test set (gray line). Since the 100-sample test set of digits is unknown to the algorithm during training with the 100-sample training set, the increase in the success rate on the test-set suggests that generalization is achieved in this approach, i.e. discrepancies between different hand-written versions of the same digit do not prevent a correct classification. While 40% success rate appears low for existing classical machine-learning models, this first proof of principle of an optically trained atom still surpasses the 10% random-guessing result by a factor of 4.

In summary, we have introduced a novel concept of optically programmable learning using quantum states for classification. As a proof of principle, the concept was applied to hand-written pixel-drawn digit recognition, implemented with a few-level model of an atom and a straightforward encoding of input/data and program/code by spectral phase functions of two orthogonally polarized femtosecond optical laser fields. Once the optimal program pulse is known, the digit recognition code runs on the femtosecond time scale, which is much faster than the processing time of any classical or quantum computer. The ultrafast time



evolution minimizes the influence of environment-induced decoherence and makes the proposed scheme robust. We note that replacing the atom by a larger quantum system, such as a complex molecule, enormously increases the size of the Hilbert space while preserving the ultrafast time scale. We have chosen the digit-recognition task as it is routinely used in conventional machine learning and we run it on a simple quantum system for which the TDSE can be solved numerically. For more complex tasks implemented on larger systems, the numerical solution of the TDSE becomes prohibitive so that the actual experiment becomes the method of choice. In this study, we have achieved a recognition rate of 40% based on a very limited training set and minimal computational resources. The following strategies to improve the performance of the method are conceivable: (a) Parameterization of the data pulse: one could imagine a pixel to pulse-shape mapping preserving the essential features of the pulse for a given digit upon translation and/or scaling. (b) Parameterization of the code pulse: introducing more parameters into the spectral phase function provides more flexibility in the code pulse. However, this increases the search space, which requires more computing power. (c) More adapted/advanced optimization methods will reduce the training time and lead to higher recognition rates by exploring the parameter space more comprehensively. (d) More computational resources to implement all the above enhancements. Training refinements include much larger training sets, higher dimensional code-parametrizations, more iterations, etc.

The key advantage of our approach is based on the versatility of possible applications using the same quantum system as computational kernel. For example, future applications could include other computational tasks, such as identifying letters, images, or prime numbers. In our approach, the quantum system acts as an optically reprogrammable general-purpose quantum processor. While here we only introduce and explore the key idea by means of a one-particle few-level model, future experimental implementations will involve few- or many-body dynamics to employ a much larger state space and thus higher effective number of coupled layers of states (neurons). A crucial point that distinguishes this scheme from existing quantum-computing approaches and platforms is the fact that (entangling) operations are not

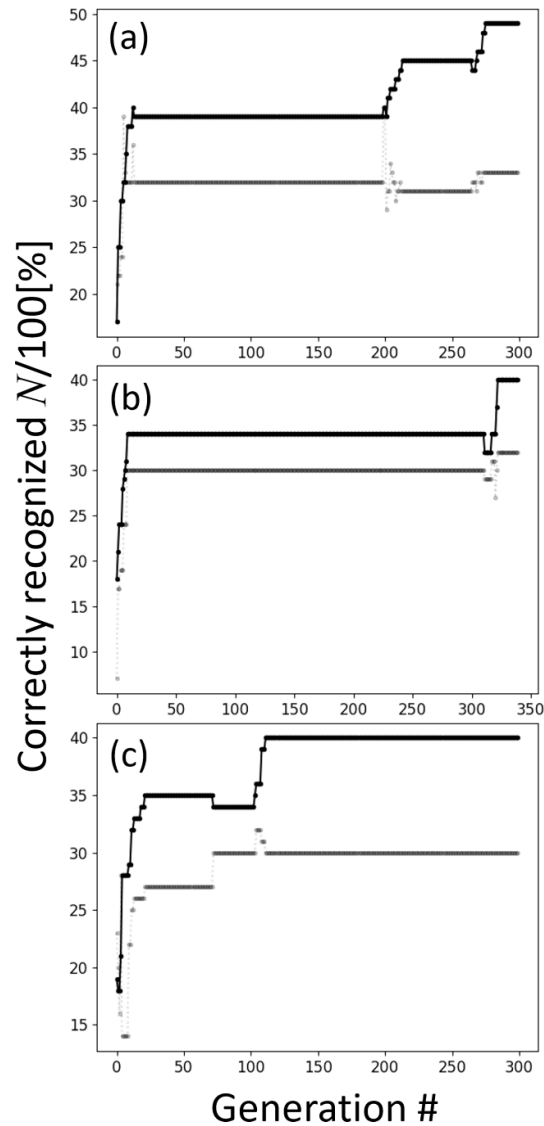


Figure 4. Percentage of correctly recognized digits for three example runs of the evolutionary algorithm to optimize the program fields for digit recognition. (a) Model with state-independent couplings a for all transitions, (b) model with state-dependent couplings $a' = a/(|n - n'| + 1)$, (c) model with modified state energies $E_{nl} = -2.16/(n + 2)^2$. Black points: fittest individual when applied to the training set. Grey points: fittest individual when applied to an (unseen) test set for validation of the generalization of learning. Routinely, success rates of $> 40\%$ and $\sim 30\%$ are achieved for training and test sets, respectively.

performed on spatially *separated* entities but on *compact* quantum systems of interacting particles. It is therefore neither possible nor necessary to implement traditional quantum gates. Instead, suitably-shaped structured light pulses are used to perform the operations required for the envisaged task. The use of ultrafast polarization shaping to transfer the data and the code into an atomic-scale quantum system as well as the execution within the system proceeds on femtosecond time scales, implying unprecedented speed when compared to classical computers as well as quantum computers using trapped ions or superconducting qubits. Therefore, this approach may lead to new scientific as well as technological applications, for example in real-time classification. It has the potential to outpace other currently implemented machine-learning approaches, including the fastest optical on-chip neuromorphic systems and optical accelerators, by orders of magnitude. The experimental implementation of the scheme is possible using ultrafast polarization pulse shaping to implement the id- and pc-pulses, and employing photoelectrons to map the final population of classification states [37]. Multi-electron systems with larger Hilbert spaces, realized as multi-electron atoms, molecules or solid-state samples provide additional computational resources, e.g. correlation and entanglement. Therefore, these systems are expected to be even more effective for the presented ultrafast laser-driven approach.

Our scheme can be viewed as a form of machine learning with a microscopic quantum system. Similar to classical machine learning, there is not necessarily a simple explanation for how the trained machine makes its decisions. Finding the optimal external program field to control the atom based on a cumulative reward

(here: recognizing as many digits as possible) can be viewed as a reinforcement learning concept, providing an exciting future avenue at the intersection of these research domains. Overall we expect that ultrafast AI on the atomic scale has the potential to exploit quantum mechanics for high-speed computational tasks in the future.

Data availability statement

The data cannot be made publicly available upon publication because they are not available in a format that is sufficiently accessible or reusable by other researchers. The data that support the findings of this study are available upon reasonable request from the authors.

Acknowledgments

We acknowledge support by the Deutsche Forschungsgemeinschaft (DFG, German Research Foundation) under Germany's Excellence Strategy EXC2181/1-390900948 (the Heidelberg STRUCTURES Excellence Cluster) and the Priority Programme *Quantum Dynamics in Tailored Intense Fields* (QUTIF).

ORCID iDs

Thomas Pfeifer  <https://orcid.org/0000-0002-5312-3747>

Matthias Wollenhaupt  <https://orcid.org/0000-0002-0839-1494>

Manfred Lein  <https://orcid.org/0000-0003-1489-8715>

References

- [1] Goodfellow I, Bengio Y and Courville A 2016 *Deep Learning* (MIT Press)
- [2] Trask A W 2019 *Grokking Deep Learning* (Manning)
- [3] Plamondon R and Srihari S N 2000 Online and off-line handwriting recognition: a comprehensive survey *IEEE Trans. Pattern Anal. Mach. Intell.* **22** 63–84
- [4] Vapnik N V 1998 *Statistical Learning Theory* (Wiley)
- [5] Neyshabur B, Bhojanapalli S, McAllester D and Srebro N 2017 Exploring generalization in deep learning *Advances in Neural Information Processing Systems 30 (Curran Associates, Inc.)* (available at: https://proceedings.neurips.cc/paper_files/paper/2017/file/10ce03a1ed01077e3e289f3e53c72813-Paper.pdf)
- [6] Kawaguchi K, Kaelbling L P and Bengio Y 2022 Generalization in deep learning *Mathematical Aspects of Deep Learning* (Cambridge University Press)
- [7] Feldmann J, Youngblood N, Wright C D, Bhaskaran H and Pernice W H P 2019 All-optical spiking neurosynaptic networks with self-learning capabilities *Nature* **569** 208–14
- [8] Ashtiani F, Geers A J and Aflatouni F 2022 An on-chip photonic deep neural network for image classification *Nature* **606** 501–6
- [9] Weinacht T C, Ahn J and Bucksbaum P H 1999 Controlling the shape of a quantum wavefunction *Nature* **397** 233–5
- [10] Ott C et al 2014 Reconstruction and control of a time-dependent two-electron wave packet *Nature* **516** 374–8
- [11] Pengel D, Kerbstadt S, Johannmeyer D, Englert L, Bayer T and Wollenhaupt M 2017 Electron vortices in femtosecond multiphoton ionization *Phys. Rev. Lett.* **118** 053003
- [12] Jiang W et al 2022 Atomic partial wave meter by attosecond coincidence metrology *Nat. Commun.* **13** 5072
- [13] Kretschmar M, Hadjipittas A, Major B, Tümmler J, Will I, Nagy T, Vrakking M J J, Emmanouilidou A and Schütte B 2022 Attosecond investigation of extreme-ultraviolet multi-photon multi-electron ionization *Optica* **9** 639–44
- [14] Yu M et al 2022 Full experimental determination of tunneling time with attosecond-scale streaking method *Light Sci. Appl.* **11** 215
- [15] Meister S et al 2021 Linear dichroism in few-photon ionization of laser-dressed helium *Eur. Phys. J. D* **75** 205
- [16] Akoury D et al 2007 The simplest double slit: interference and entanglement in double photoionization of H₂ *Science* **318** 949–52
- [17] Schöffler M S et al 2008 Ultrafast probing of core hole localization in N₂ *Science* **320** 920–3
- [18] Vrakking M J J 2021 Control of attosecond entanglement and coherence *Phys. Rev. Lett.* **126** 113203
- [19] Koll L M, Maikowski L, Drescher L, Witting T and Vrakking M J J 2022 Experimental control of quantum-mechanical entanglement in an attosecond pump-probe experiment *Phys. Rev. Lett.* **128** 043201
- [20] Laurell H et al 2022 Continuous-variable quantum state tomography of photoelectrons *Phys. Rev. Res.* **4** 033220
- [21] Shobeiry F, Fross P, Srinivas H, Pfeifer T, Moshhammer R and Harth A 2024 Sub-femtosecond optical control of entangled states *Sci. Rep.* **14** 19630
- [22] McCaul G, Jacobs K and Bondar D I 2023 Towards single atom computing via high harmonic generation *Eur. Phys. J. Plus* **138** 123
- [23] Biamonte J, Wittek P, Pancotti N, Rebentrost P, Wiebe N and Lloyd S 2017 Quantum machine learning *Nature* **549** 195–202
- [24] Beer K, Bondarenko D, Farrelly T, Osborne T J, Salzmann R, Scheiermann D and Wolf R 2020 Training deep quantum neural networks *Nat. Commun.* **11** 808
- [25] Tesch C M and de Vivie-Riedle R 2002 Quantum computation with vibrationally excited molecules *Phys. Rev. Lett.* **89** 157901
- [26] Palao J P and Kosloff R 2002 Quantum computing by an optimal control algorithm for unitary transformations *Phys. Rev. Lett.* **89** 188301
- [27] Teranishi Y, Ohtsuki Y, Hosaka K, Chiba H, Katsuki H and Ohmori K 2006 Implementation of quantum gate operations in molecules with weak laser fields *J. Chem. Phys.* **124** 114110
- [28] Ahn J, Weinacht T C and Bucksbaum P H 2000 Information storage and retrieval through quantum phase *Science* **287** 463–5
- [29] Liu Y, Arunachalam S and Temme K 2021 A rigorous and robust quantum speed-up in supervised machine learning *Nat. Phys.* **17** 1013–7

- [30] Sharma D, Singh P and Kumar A 2023 The role of entanglement for enhancing the efficiency of quantum kernels towards classification *Physica A* **625** 128938
- [31] Judson R S and Rabitz H 1992 Teaching lasers to control molecules *Phys. Rev. Lett.* **68** 1500–3
- [32] Russell S J and Norvig P 2021 *Artificial Intelligence: A Modern Approach* (Pearson)
- [33] Feit M D, Fleck J A Jr and Steiger A 1982 Solution of the Schrödinger equation by a spectral method *J. Comput. Phys.* **47** 412–33
- [34] Bandrauk A D and Shen H 1992 Higher order exponential split operator method for solving time-dependent Schrödinger equations *Can. J. Chem.* **70** 555–9
- [35] Bauer D (ed) 2017 *Computational Strong-Field Quantum Dynamics: Intense Light-Matter Interactions* (De Gruyter)
- [36] Simon D 2013 *Evolutionary Optimization Algorithms: Biologically-Inspired and Population-Based Approaches to Computer Intelligence* (Wiley)
- [37] Braun H, Bayer T, Pengel D, Wollenhaupt M and Baumert T 2017 Simultaneous observation of transient and final state dynamics in ultrafast strong-field excitation via time-resolved photoelectron spectroscopy *J. Mod. Opt.* **64** 1042–53